Engineering Chemistry
ISSN: 2813-6535, Vol. 9, pp 33-51
doi:10.4028/p-Sv736e

Submitted: 2024-09-27
Revised: 2024-12-03
Accepted: 2024-12-11
Online: 2025-03-10

Direct Electron Transfer and Electro-Catalytic Activity of Non-Enzymatic Glucose Biosensor Based on Silver Nanoparticle (AgNPS) Stabilized with Sodium Tripolyphosphate (NaTPP) Cross-Linked Chitosan

Akeem Adesina Bamigbade[1a*], Enock Olugbenga Dare[1b],
Biodun S. Badmus[2c] and Janet Titilayo Bamgbose[1d]

[1]Chemistry Department, Federal University of Agriculture Abeokuta

[2]Physics Department, Federal University of Agriculture Abeokuta

[a*]bamigbadeaa@funaab.edu.ng, [b]dareeo@funaab.edu.ng, [c]badmusbs@funaab.edu.ng,
[d]bamgbosejt@funaab.edu.ng

Keywords: Silver nanoparticle; Sodium tripolyphosphate; Glucose; Characterization; Electrochemical, Sensor

Abstract. The development of non-enzymatic glucose biosensor has been the concern of many researchers mainly because enzymes based sensor despite having excellent sensitivity and selectivity, has the limitations such as poor stability, complicated enzyme immobilization, critical operating conditions such as optimum temperature and reproducibility. This study developed a cheap biocompatible non-enzymatic glucose biosensor based on silver nanoparticle (AgNPs) stabilized with sodium tripolyphosphate (NaTPP) cross-linked chitosan. Direct electron transfer and electro-catalytic activity of the AgNPs modified glassy carbon electrode (AgNPGCE) was investigated using potentiometric and amperometric techniques. AgNPs was prepared and characterized by Fourier transform Infra-red spectroscopy (FTIR), X-ray diffractometry (XRD) and Scanning electron microscopy (SEM). The crystalline size of the AgNPs was revealed with XRD. However, the SEM micrograph of AgNPs revealed the spherical shape with a non-uniform granular shape attributed to bio-mediated ionic gelation process. The FTIR spectra of AgNPs shown peaks at 1054 – 1645 cm^{-1} suggesting the presence of phosphonate linkages between ammonium, $-NH_3^+$ of chitosan and $–PO_3^{2-}$ moieties of NaTPP during cross linking process. Electro-catalytic oxidation of glucose at the AgNPGCE surface and the mechanism involved in glucose oxidation was revealed via cyclic voltammetry. The AgNPGCE showed a better electrochemical response towards glucose. This glucose sensor showed high sensitivity at +0.54 V. A low detection limit of 1.22 μM (the confident level $k = 3$), and wide linear range of 2 to 24 μM with a correlation coefficient of 0.9987 were obtained. The calculated parameters revealed that AgNPGCE had shown better overall electrochemical performance and response than enzymatic biosensor.

Introduction

Diabetes mellitus is a protracted disease that occurs when the pancreas fails to produce enough insulin to regulate blood sugar or when the body is incapable to use the insulin produced efficiently. Failure to treat diabetes effectively, will largely result into a number of other health complications, such as eye problems (blindness), neuropathy, foot complications, kidney disease, heart diseases, hypertension, stroke, hyperglycemic nonketonic syndrome, gastroparesis, heart disease, and mental health disorders; death and disability in the entire globe, it may also affect pregnancy [1, 2]. Glucose ($C_6H_{12}O_6$) is an essential energy-providing substance in life, but excessive glucose concentration in the body can result into many severe and even life-threatening diseases, such as diabetes [3]. Particularly, accurate glucose measurement for diabetics is an effective tool in the detection and treatment of diabetes mellitus [4].

For diabetic patients, a normal blood glucose level in human serum before a meal is around 4 – 6 mM (70 – 110 mg/dL) and < 7.8 mM (< 140 mg/dL) after 2 hours of mealtime [5]. Regular testing of physiological blood glucose levels is necessary to avoid diabetic emergencies and is crucial for the confirmation of effective treatment [6]. For effective therapy and to prevent any hyperglycemia or hypoglycemia, regular monitoring of physiological blood glucose levels is crucial.

Therefore, researchers have been looking for fast, accurate and steady methods to determine glucose levels in vivo and in vitro [7]. Glucose sensors with high sensitivity, high stability and high accuracy produced by optical [8], electrochemical [9] and other techniques are of great importance in blood glucose monitoring of diabetic patients. The detection of blood glucose is of great significance in the food process application, clinical medicine, and biology [10, 11]. Therefore, the production of high sensitive, low-cost, reliable glucose sensors having an outstanding selectivity has been the subject of interest for decades, not only in medical science but also in the food industries [12]. Glucose oxidase (GOx)-based glucose biosensors have prevalently dominated the glucose sensor research and development over the last four decades and the market place as well. This is due to the increasing demand of sensitive and reliable blood glucose monitoring in biological and clinical aspects [13-15]. Enzymes based sensor displays excellent sensitivity and selectivity.

The main restrictions to these sensors are poor stability and reproducibility, which can impede the sensor properties. Apart from deactivation of the enzyme some other disadvantages of enzyme-based glucose determination includes complicated enzyme immobilization, critical operating conditions such as optimum temperature and pH, chemical instability, and high cost [4, 16].

Electrochemical sensing techniques are versatile and powerful tools in providing real time and on-site measurement in a variety of areas, including clinical diagnostic, environmental, agricultural, and food monitoring [17-19]. The electrochemical sensing offers advantages in providing high sensitivity, selectivity, accuracy, and cost effectiveness.

Therefore, non-enzymatic glucose sensors developed mainly based on creation of electrode surface by direct oxidation of glucose without the help of enzyme, which had sustainable advantages in terms of simplicity, manufacturability, portability, selectivity, stability, sensitivity and their low cost [20-22]. Non-enzymatic glucose biosensors can escape that problem because of direct catalytic oxidation of glucose on the surface of electrode [20, 21].

In order to increase specific surface areas and improve mass transport ability, these electrodes could use nanomaterials as substrates like carbon nanotubes (CNTs) [22], nanowires [23, 24], meso porous structure [25], etc., and modified with mental nanoparticles such as Pt [26], Ni [27], Ag [28], and Cu [29]. In the present research, we want to investigate the synthesis of silver nanoparticles by an environmental friendly procedure involving the in situ reduction of silver (Ag) and to investigate the electrocatalytic activity of silver nanoparticle stabilized by chitosan on oxidation of glucose in order to explore the possibility of developing biosensor that will respond to glucose measurement in any system.

Experimental Procedure

Apparatus

Electrochemical measurements were carried out with a potentiostat/ galvanostat with a single compartment Voltammetric cell coupled to a computer, equipped three electrodes: glassy carbon electrode as working electrode with dimension of 5.0mm diameter and 8.0mm length, an electrical contact provided by a copper wire, an Ag/AgCl (with 3M KCl) reference electrode of 4.0 mm diameter, a copper wire contact, and a platinum wire acting as the counter electrode (diameter of 0.5 mm). An ultrasonic bath, magnetic stirrer and a Thermostarted bath were also used.

Reagents

Chitosan produced from lobster shell wastes with 85% degree of deacetylation was purchased from Aldrich and used as supplied. Hydrochloric acid, glacial acetic acid and Sodium hydroxide, were supplied by Aldrich. Sodium borohydride($NaBH_4$), sodium tripolyphosphate (NaTPP), Silver nitrate ($AgNO_3$), $\beta-$D$-$glucose, acetone and Ethanol were obtained from Sigma Chemical and Co and used as received.

All solutions were prepared with double distilled water, and all chemicals were used without further purification. All the experiments were carried out at ambient temperature of 25 ± 1 °C.

Preparation and characterization of silver-chitosan Nanoparticle (AgNPs)

A silver-chitosan nanoparticle (AgNPs) was prepared according to a modified literature procedure [30-32].

60mg chitosan was dissolved in 20 mL of 2% acetic acid to obtain chitosan solution. 5% of NaTPP solution was added to chitosan solution in the ratio of 1:3 NaTPP to chitosan, with mild stirring until an opalescent suspension was obtained. 10 mL of 0.35% of silver nitrate solution was added to the chitosan-NaTPP hydrogel and stirred continuously for 30 minutes to obtain homogeneous solution.

Final stage of the synthesis was the addition of 10 mL of 0.01 M sodium borohydride (reducing agent). $AgNO_3$/Chitosan- NaTPP gelatine is a colourless solution, but once the reducing agent $NaBH_4$ was introduce to the polymer suspensions, there was immediate colour change to dark brown, indicating the formation of silver nanoparticle [30, 32]. The chitosan-silver nanoparticle was separated from the liquid by centrifugation for one hour at 10,000 g. The supernatant was discarded and the particles were washed thoroughly with acetone, ethanol, distilled water and then vacuum filtered. The obtained particles were oven-dried at 110 ºC.

The silver nanoparticle prepared was characterized using Fourier-transformed Infra-red spectroscopy (FTIR), X-ray diffractometer (XRD), Ultraviolet-visible spectrophotometer, and Scanning electron microscope (SEM).

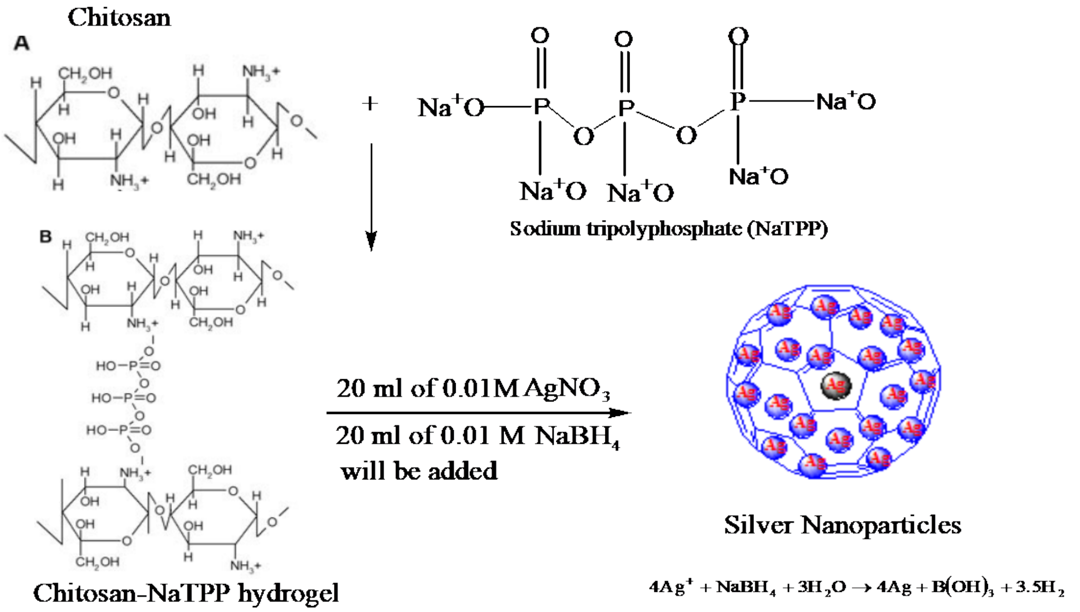

Note: The positive charges on the amino groups of chitosan resulting from its dissolution in acetic acid interact with the negative charges on the tripolyphosphate anions, causing ionic-gelation and formation of hydrogel.

Fig. 1. Schematic representation of reaction path for the preparation of the Chitosan-silver nanoparticle

Electrode preparation

The surface of the Glass Carbon Electrode (GCE) was polished with the alumina suspension using a polishing cloth to a mirror finish. The electrode surface was then cleaned in an ultrasonic bath for 15 minutes and washed with ethanol and deionized water to remove adsorbed particles [33, 34]. This procedure was repeated after each voltammetric experiment. Other materials, including glassware, containers, pipette tips and the electrochemical vessels, were washed and sterilized with heat prior to use.

Preparation of silver nanoparticle (AgNPs) modified glassy carbon electrode (GCE)

The electrode surface was uniformly coated with 2 μL of 1% silver nanoparticle solution in 1% acetic acid and air-dried, after which it was immersed in 50 μL of 0.1 M NaOH (to stabilize the silver nanoparticle) and again air-dried.

The electrochemical characteristics of silver nanoparticle-supported glassy carbon electrode

The electrochemical performance of the silver nanoparticle modified glass carbon electrode (AgNPGCE) and bare glass carbon electrode (GCE) as control was investigated in 2 mM glucose and 5 ml of 0.1M sodium hydroxide as supporting electrolyte at 150mV/s scan through cyclic voltammetry (CVs) procedure. The electro-catalytic activity of AgNPs-modified glassy carbon electrode was investigated through cyclic voltammetry using 10 mM glucose in 5 ml of 0.1 M sodium hydroxide solution, at different scan rate of 10, 25, 50 100 and 150 mV s^{-1}, with a potential window of 0.0 V and 1.0V at 0.1 Vs^{-1}.

Electro-catalytic characterization and charge transfer kinetics of AgNPs-glassy carbon electrode

Cyclic voltammetry assay of AgNPs-glassy carbon electrode was performed in air-saturated 5 ml of 0.1 M sodium hydroxide (supporting electrolyte) at room temperature at scan rate of 10 mV s^{-1} within a potential window of 0.0 V and 1.0V at 0.1 Vs^{-1}, with addition of different concentrations of glucose corresponding to (a) 2, (b) 4, (c) 6, (d) 8, (e) 10 mM [34-36].

Results and Discussion

Silver nanoparticles (AgNP) prepared from chitosan was characterized using scanning electron microscopy (SEM), X-ray diffractometry (XRD) and Fourier transform Infra-red spectroscopy (FT-IR). The SEM micrograph of silver nanoparticle derivatives were recorded and the micrograph are shown in figure 2, while the XRD and FT-IR spectra of silver nanoparticle derivatives are shown in figure 3 and 4 respectively.

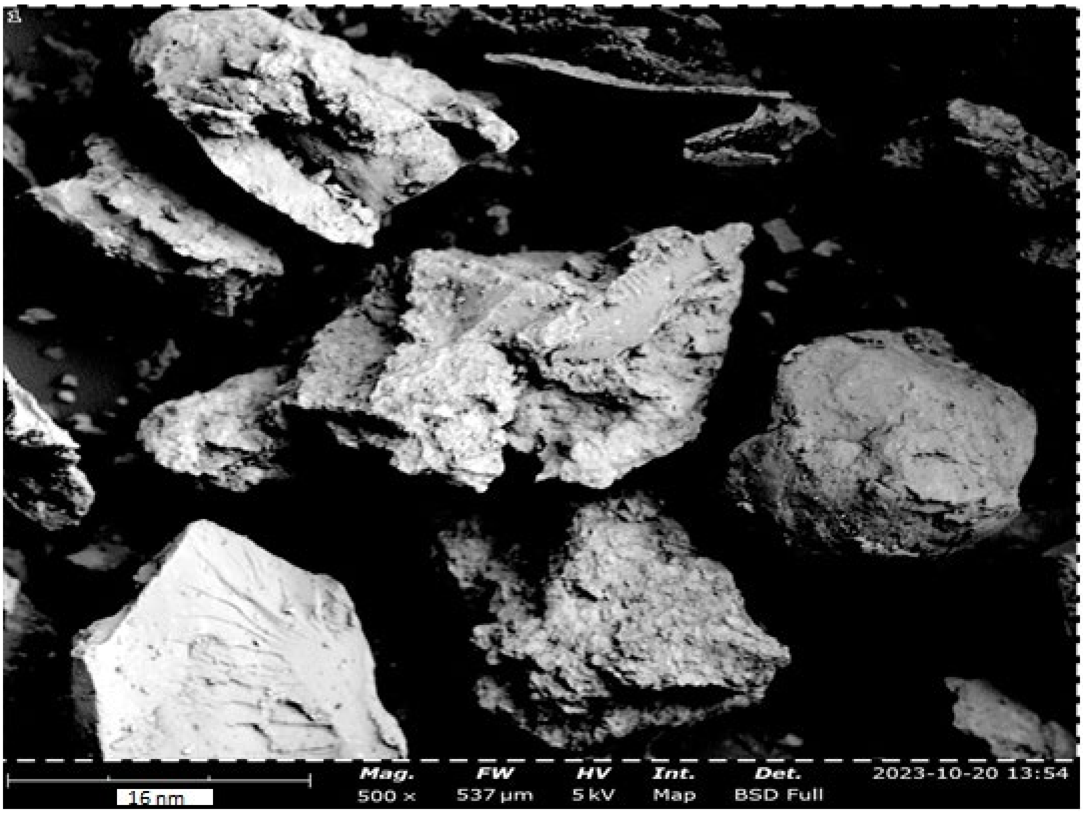

Fig. 2. Scanning Electron Micrograph (SEM) of AgNPs

The morphological features of silver nanoparticles derivatives were studied by NOVA Nano - Scanning Electron Microscope (JSM - 6480 LV). The SEM slides were prepared by making a smear of the solutions on slides. A thin layer of platinum was coated to make the samples conductive. Then the samples were characterized in the SEM at an accelerating voltage of 5 KV, emission current of 75 – 80 A and working distance of 6 – 13 nm. The particle morphology was determined via SEM analysis. Silver nanoparticles image enlargement was carried out on a scale of 150 μm with HV 5.0 Kv as presented in figure 2 above. The surface morphology of the silver nanoparticle morphology presented in figure 2 shows a relatively spherical shape, high density structure with a non-uniform granular shape credited to bio-mediated ionic gelation process. The surface of the synthesized silver nanoparticles has a spherical shape and slightly elongated with a big propensity to aggregate and form larger particle clusters.

XRD Analysis

The phase variety and grain size of synthesized silver nanoparticles was determined by X-ray diffraction Spectroscopy (Philips PAN analytical). The synthesized nanoparticle was studies with Cu-Kα radiation at voltage of 30 kV and current of 20 mA with scan rate of 0.03 0/s, λ = 1.54 Å.
Figure 3 presents XRD spectra of silver nanoparticle derived hybrid. The XRD spectrum of silver nanoparticle in figure 3 shows that silver nanoparticles have been formed. The structures of synthesized silver nanoparticles confirm the cubic face-centered structure of silver nanoparticle. This was supported by the observed sharp four diffraction peaks with peaks intense appeared at 2θ = 38.09°, 44.15°, 64.67°, and 77.54° as shown in figure 3 which are indexed to 111, 200, 220, and 311 Bragg's reflection [37], respectively. This confirms the crystalline structure of silver nanoparticles. The data obtained was matched with JCPDS card no. (65-2871) and the sharpness of the peak clearly reveals the crystalline nature of the particles. The crystallite size of the obtained silver nanoparticles were calculated to be 16 nm applying Debye-Scherrer Equation ($D = k\lambda/\beta\cos\theta$) with a relative deviation of 4.65%, where D is the average crystallite size of the nanoparticles, k is the geometric factor called Scherrer constant with a value of 0.9. λ is the wavelength of X-ray radiation source (0.15406 nm), θ is the Bragg's angle and β is the angular full-width at half maximum (FWHM = 0.004) of the XRD peak at the diffraction angle θ [38]. XRD patterns (JCPDS, File No. 04–0783) and the structure of synthesized silver nanoparticles were found to be face-centered cubic (FCC) crystal as reported by [39].

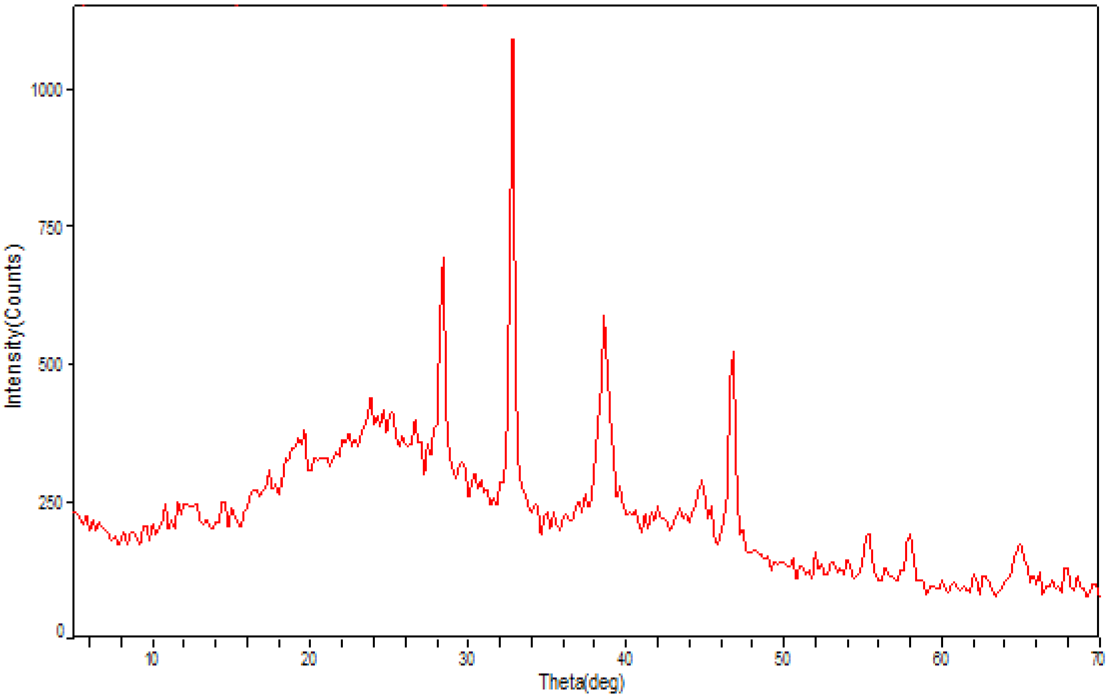

Fig. 3. XRD spectrum of Silver Nanoparticle (AgNPs)

FTIR Analysis

The FTIR spectra of silver nanoparticle derivative are shown in figure 4. Silver nanoparticle spectrum gave peaks at 1054 – 1645 cm^{-1} signifying the presence of phosphonate linkages between ammonium, $-NH_3^+$ of chitosan and $–PO_3^{2-}$ moieties of NaTPP during cross linking process. The spectrum showed two peaks, one at 1140 cm^{-1} and another at 1279 cm^{-1}, indicating symmetric and asymmetric stretching of phosphonate linkage, respectively [40]. It was also observed that the asymmetric peak is known to occur due to restricted rotation [41]. The two terminals $–PO_3^{2-}$ groups of NaTPP molecule appears to be connected with two $-NH_3^+$, (CH_3COO^-) groups of two chitosan monomers.

Meanwhile the spectrum of silver nanoparticle display a broadening of the band starting at approximately 3500 cm^{-1} and extending to and almost obscuring the CH_2 stretching region around 2900 cm^{-1}. There is also and a loss of the small features on the band. This broadening is suggestive of increased intermolecular hydrogen bonding between NH and OH. A maximum at approximately 3880 cm^{-1} is exhibited by the silver nanoparticle. This band broadening is similar to that found in the literature for chitosan-NaTPP nanoparticles and for chitosan succinlyated nanoparticles [42] and is ascribed to the formation of hydrogen bonded networks. The AgNPs show a low intensity but very broad band centred around 3263 cm^{-1}. This observation suggests that silver chitosan complexes prepared contain mostly nanoparticles.

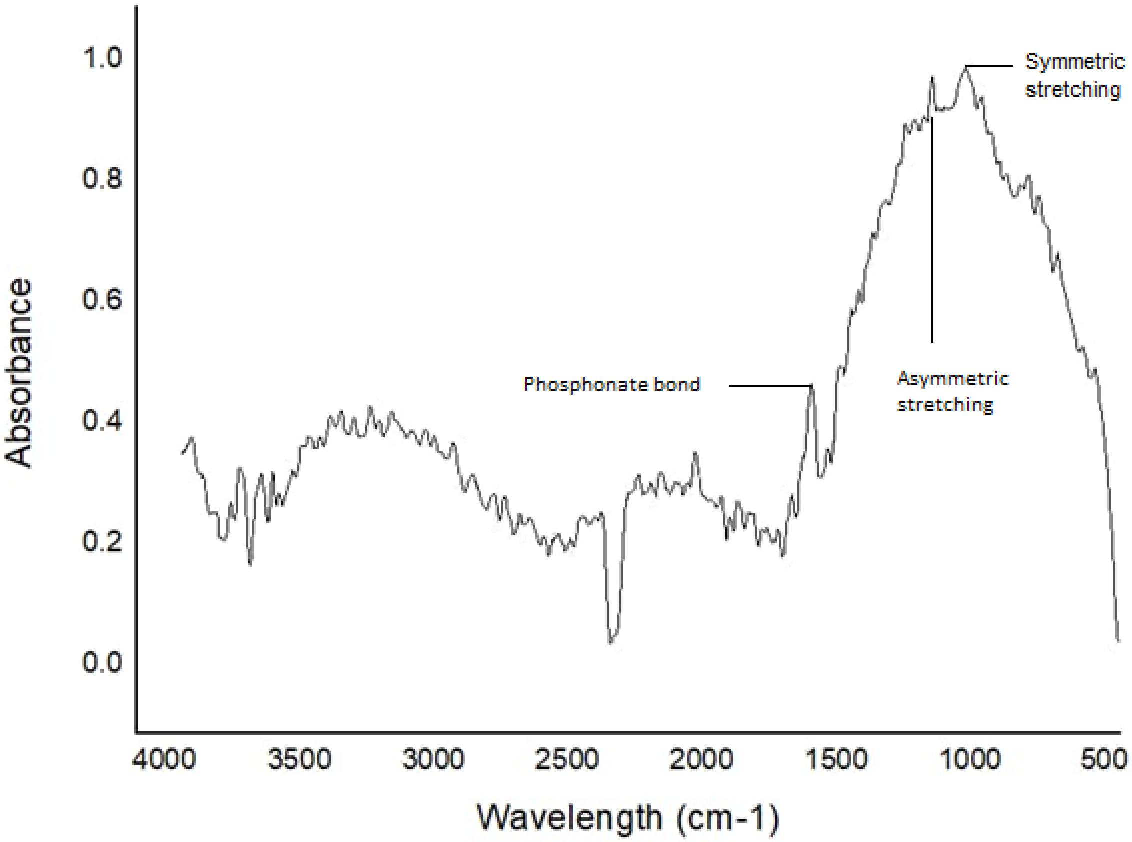

Fig. 4. FTIR spectrum of Silver Nanoparticle (AgNPs)

UV-Visible Analysis

The brown colored silver nanoparticle solution that formed due to excitation of surface Plasmon vibrations of the silver nanoparticles was subjected to UV-Visible spectra recording using Shimadzu UV-1601 double beam spectrometer with quartz cuvettes of 1cm path length. The UV-Visible spectrum of AgNPs is presented in figure 5. Surface Plasmon Resonance (SPR) peak of AgNPs which is an equivalent of maximum absorbance peak occurred at around 420 nm. Previous report confirmed that AgNPs with size range 7-10 nm mostly show the SPR peaks at 420 nm as reported by Modrzejewska et al 2010 [43].

The absorbance and broadening of the peak at around 420 nm shows that the particles were mono-dispersed and indicating the surface plasmon resonance (SPR) absorption band as a result of combined vibration of electrons in resonance with UV-visible light [44-46]. The overall observations suggest that the bio reduction of (silver ions) Ag^+ to Ag^0 was confirmed by UV-Visible spectroscopy.

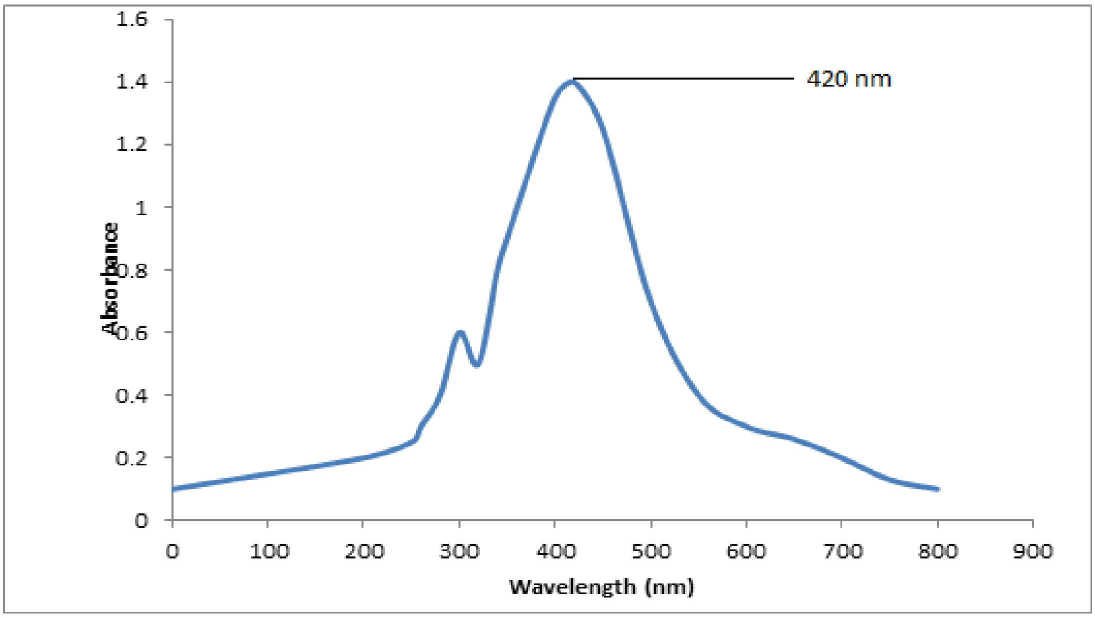

Fig. 5. UV-visible spectrum of Silver Nanoparticle (AgNPs)

Comparison Of Bare Glassy Carbon Electrode (DCE) And Silver Nanoparticle Modified Glassy Carbon Electrode (AgNPGCE)

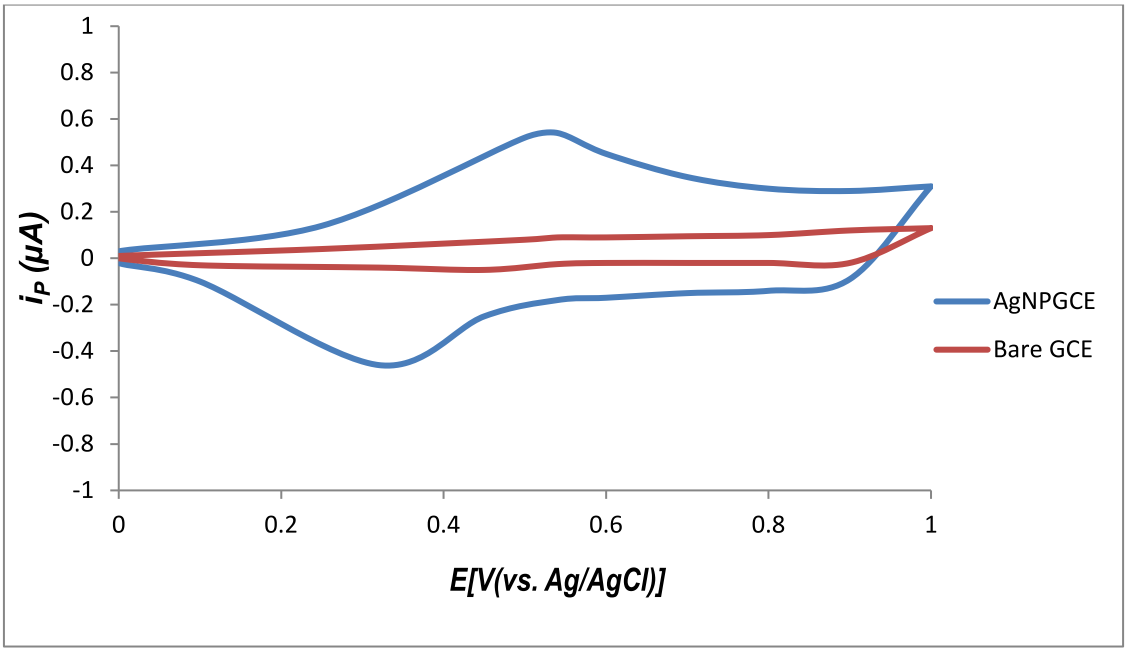

Fig. 6. Cyclic voltammograms of silver nanoparticle modified glass carbon electrode (AgNPGCE) and bare glass carbon electrode (GCE) in the presence of 2 mM glucose and 150 mV/s scan rate.

Figure 6 shows the cyclic voltammograms (CVs) of the bare GCE and AgNPGCE with glucose recorded in 0.1 M sodium hydroxide at a scan rate of 150 mVs^{-1}. The bare GCE did not give any noticeable redox peaks in the potential range recorded. However, high catalytic activity with an observable redox peaks against glucose oxidation in the alkaline solution was found for AgNPGCE compared to the bare GCE due to the increase in the active surface area of the electrochemically modified electrode as offered by the AgNPs attached to the GCE which suggest that the prepared electrode can be useful for glucose sensing phenomena [47, 48]. The AgNPs modified electrode exhibited an improved electrochemical reactivity, only one anodic peak at +0.54 V (vs. Ag/AgCl) was observed, which represent the oxidation of Ag^0 to Ag^+, while a cathodic peak at 0.32V was also noticed and may be connected with the reversible conversion of Ag^+ back to Ag^0. The electrochemical redox phenomena of Ag/Ag^+ which occur at the working electrode surface in a basic solution can be represented as

$$Ag + OH^- \rightleftharpoons AgOH + e^-$$

An oxidation reaction was suggested by the working electrode potential covered in silver nanoparticles and the electrode kinetic reaction at the surface of the AgNPGCE is represented thus.

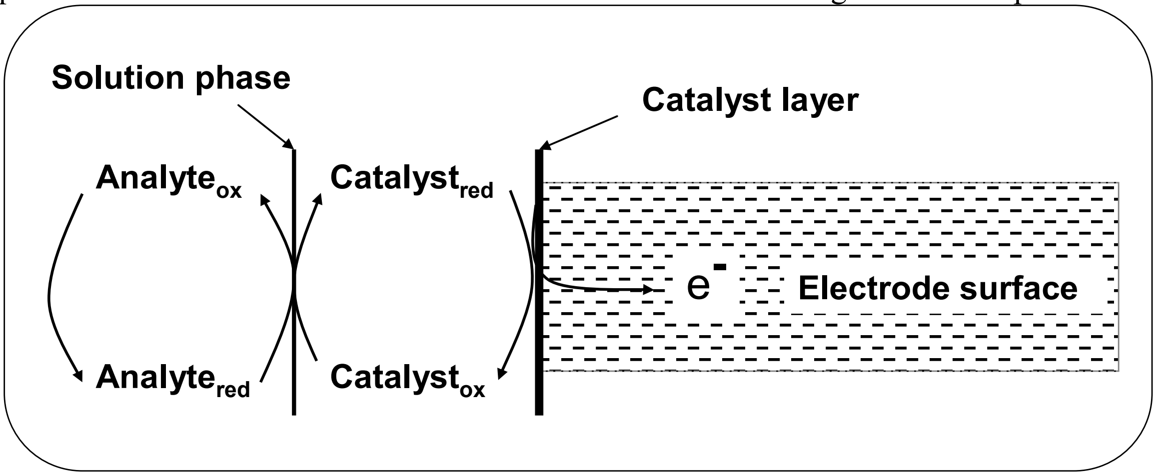

Fig. 7. Description of the mechanism of redox process at the electrode/analyte interface

This suggested that gluconolactone is produced by the glucose oxidation at the surface of AgNPGCE. The mechanism of oxidation of glucose at the AgNPGCE surface is as follow:

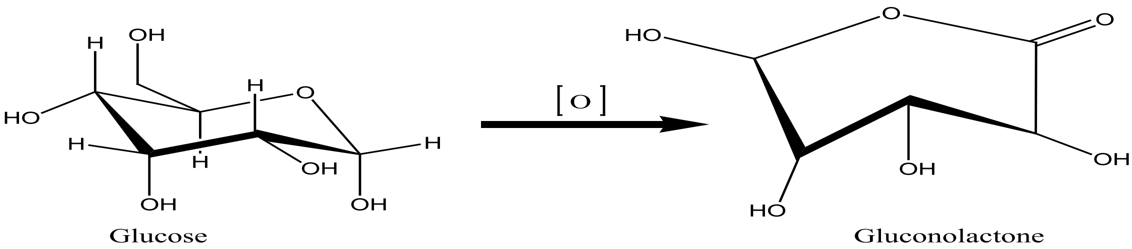

Furthermore, the existence of chitosan stabilized silver nanoparticles may increase the electrode surface area with the analyte, thereby increasing the voltage. This is because using AgNPs on the electrode facilitate increased direct electron transfer between the glucose and the electrode surface. This is because the use of silver nanoparticles on electrode could increase the direct electron transfer between the glucose and the electrode surface, adding that the presence of silver nanoparticles stabilized with chitosan could increase the surface of the electrode with the analyte thereby increasing the voltage.

Effect of Different Scan Rate on the Electrochemical Responses of Silver Nanoparticle Modified Electrode (AgNPGCE)

Figure 8 shows the cyclic voltammograms of AgNPGCE with different scan rates in 0.1 M sodium hydroxide solution containing 1 mM of glucose. The peak current (I_p) is increased with increasing scan rates 10, 25, 50 100 and 150 mVs^{-1}. As can be seen in the figure 9, the plot of I_p versus scan rates and it shows that I_p was increased linearly with increasing scan rate. The redox peak currents and peak potential separations increased with scan rates. The reduction and oxidation peak currents were directly proportional with scan rates from 10 to 150 mVs^{-1}, the result suggesting that the electrochemical kinetic is a characteristic surface-confined process i.e. the process is regulated by surface adsorption of glucose molecule at AgNPGCE [49, 50].

It can also be seen from the voltammograms that at 10 mV s^{-1}, the observed redox peaks had formal peak potential (ΔE_o) of 0.43V and peak-to-peak separation (ΔE_p) of 54.8 mV; the result was similar to previous literatures [51], which indicates reversible electrochemical reactions and rapid electron transfer process.

The anodic and cathodic peak current had a linear relationship with the square root of scan rates as shown in figure 10. The heterogeneous electron transfer rate constant (k_e) and transfer coefficient (α) were estimated using Laviron's equation [52]. The heterogeneous electron transfer rate constant (k_e) was estimated to be 6.736 x 10^{-7} cms^{-1} while the electron transfer or symmetry coefficient (α) was found to be 0.54 which is close to the theoretical value of 0.5 for reversible system. This indicates that electron transfer was effectively and efficiently promoted on the AgNPs electrode.

The surface coverage (ϕ) was found to be 3.46 x 10^{-9} $molcm^{-2}$. This value is much higher than that reported in other literatures [53, 54], suggesting AgNPs had high adsorption capacity for GCE.

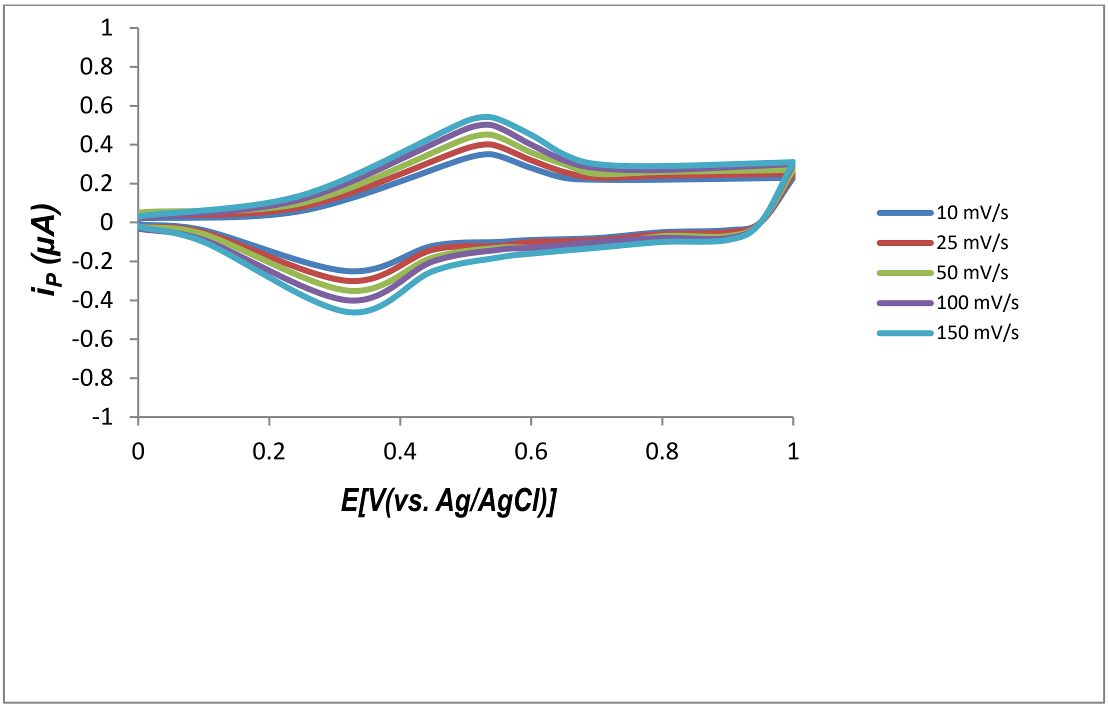

Fig. 8. Cyclic voltammograms of silver nanoparticle modified glass carbon electrode (AgNPGCE) in the presence of 2 mM glucose at different scan rate

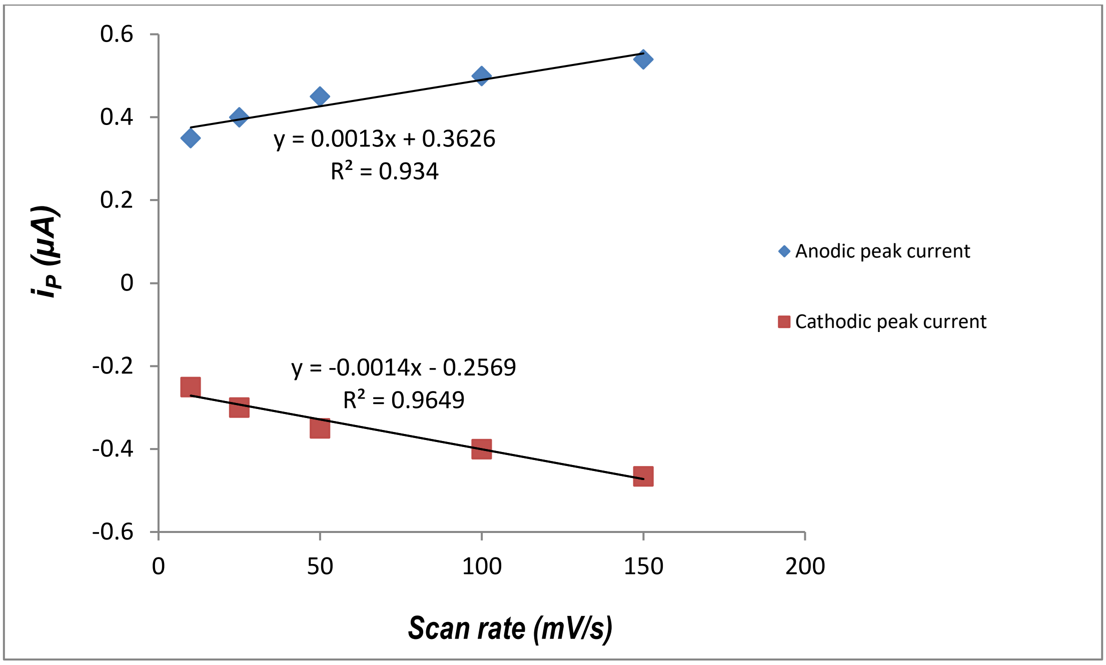

Fig. 9. Anodic and cathodic peak currents versus scan rate

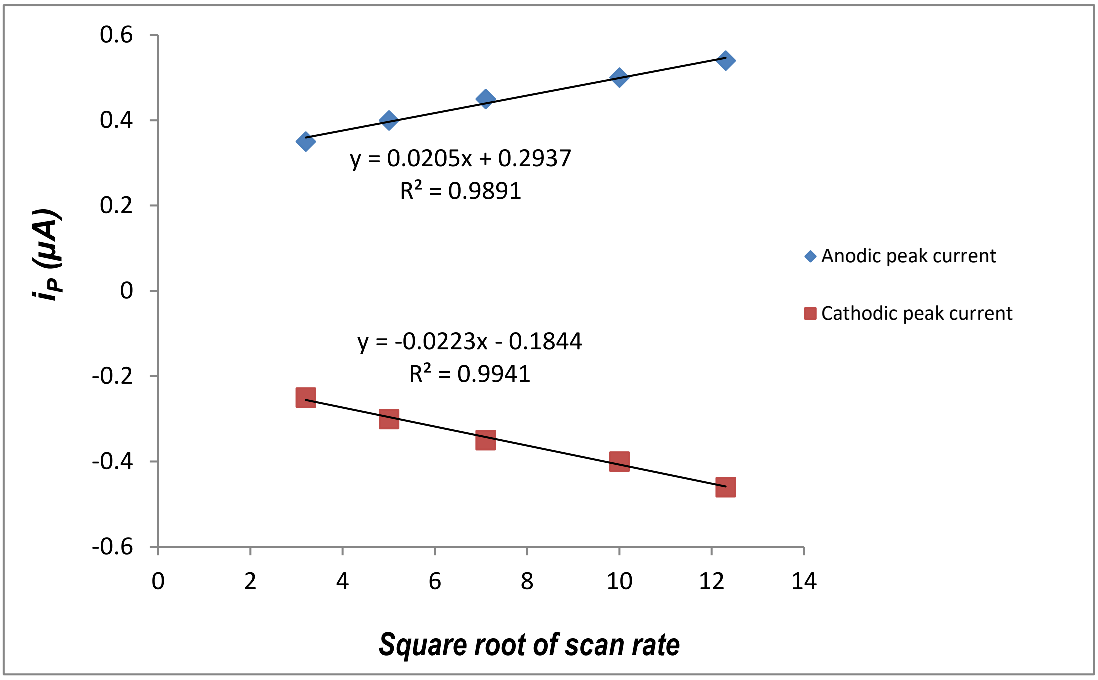

Fig.10. Anodic and cathodic peak currents versus square root of scan rate

Effect of Concentration Changes on the Electrochemical Responses of Silver Nanoparticle Modified Glassy Carbon Electrode (AgNPGCE)

Furthermore, the electron transfer capacity between electrolyte and electrode surface with the glucose concentrations ranging from 2 mM to 10 mM was investigated using cyclic voltammetry in 0.1 M sodium hydroxide solution at 10 mVs^{-1} and the result is shown in figure 11. Anodic peak at +0.54 V increases as concentration of glucose increases i.e.; peak current varied linearly in proportional to the concentration of glucose in the range of 2 – 10 mM, presented in figure 12. It can be seen from figure 6 that at every scan rate the anodic peak was observed at 0.54V, therefore, 0.54 V is chosen as the ideal detection potential. The electro-catalytic oxidation of glucose is mainly particle size dependent, which can provide the active sites for redox reaction and biological electrical signal transmission at AgNPGCE. Hence, the synergistic influence can result in enhanced performance for detection of glucose [55].

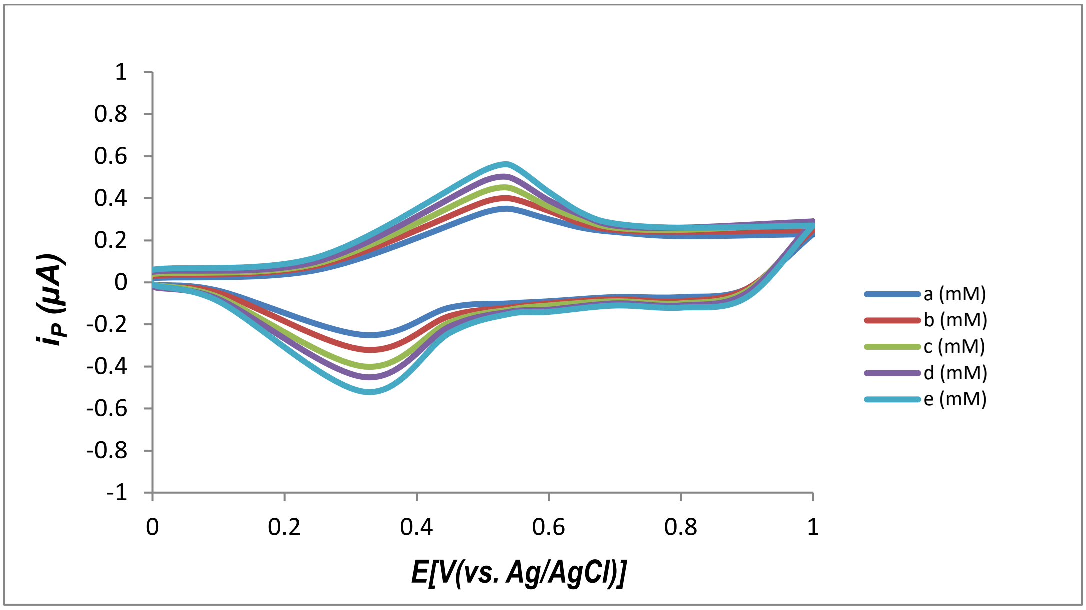

Fig. 11. Cyclic voltammograms of silver nanoparticle modified glass carbon electrode (AgNPGCE) in air-saturated NaOH (0.1M) at scan rate of 10 mVs^{-1} with the additional of 2 mM (a), 4 mM (b) 6 mM (c), 8 mM (d) and 10 mM (e)

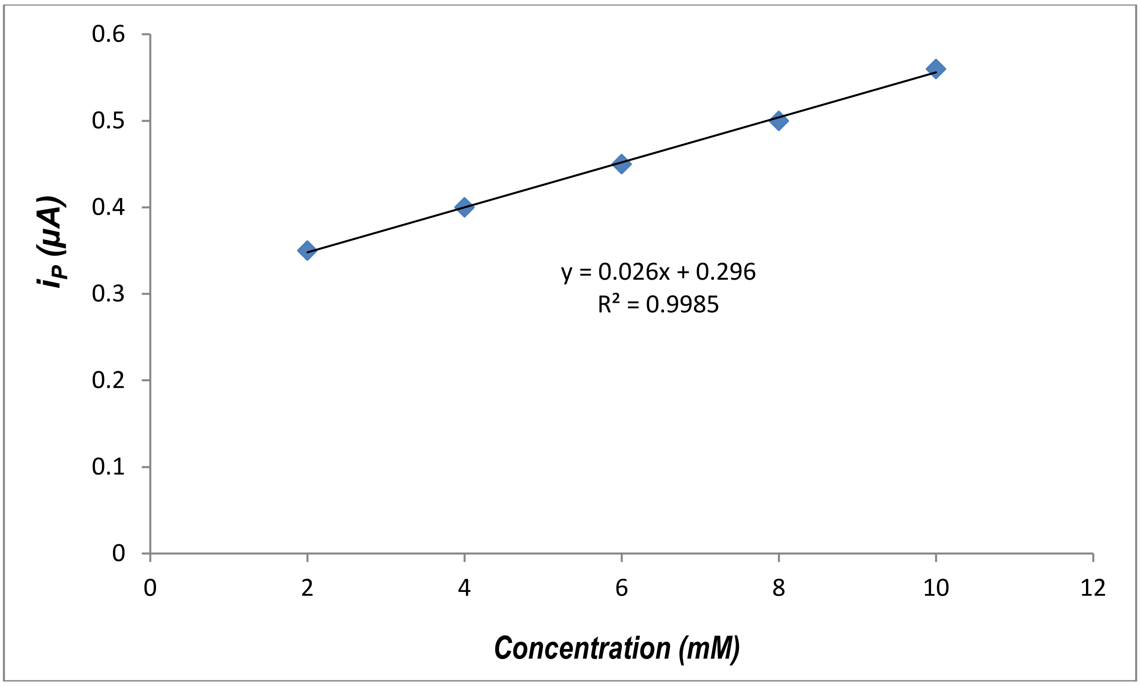

Fig. 12. Plot of relation between oxidation peak currents and concentrations of glucose

Amperiometric Detection of Glucoses

To further investigate the relationship between oxidation current and glucose concentration, the chronoamperometry technique was used and the results obtained are presented in figure 13a and 13b respectively.

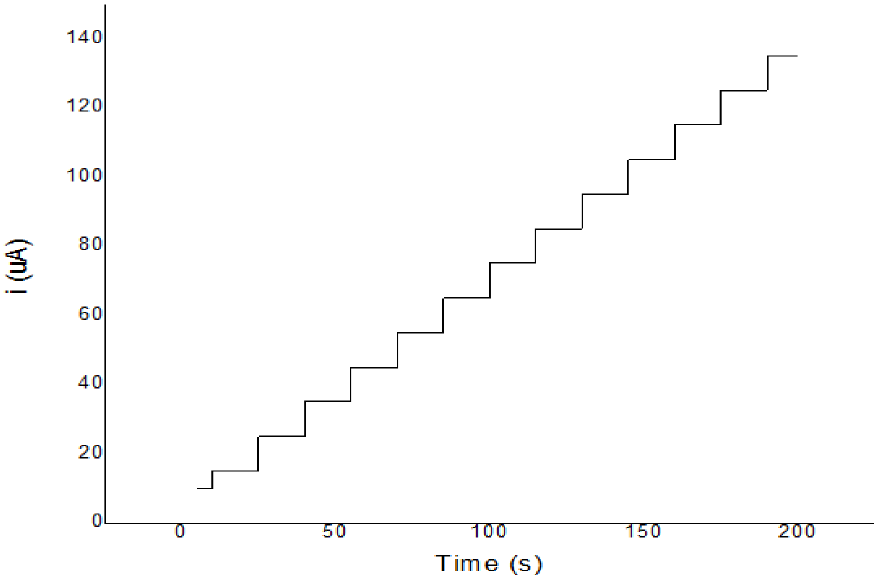

Fig. 13a. Amperometric current versus time curve of silver nanoparticle modified glass carbon electrode (AgNPGCE) for successive glucose addition in the ranges of 2 µM to 24 µM

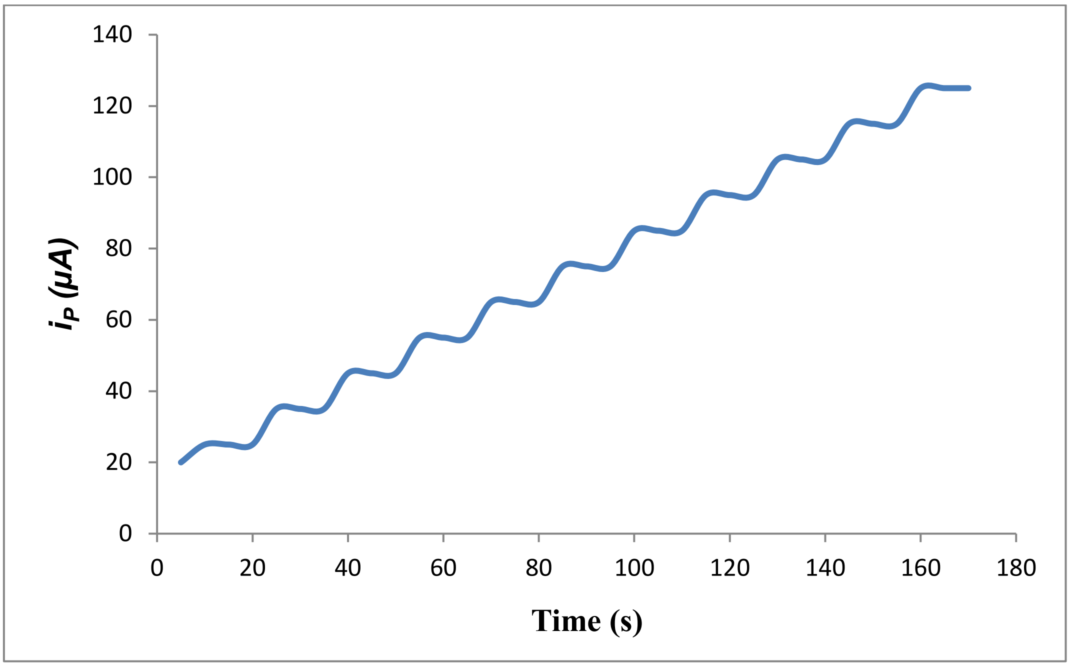

Fig. 13b. Amperometric current versus time curve of silver nanoparticle modified glass carbon electrode (AgNPGCE) for successive glucose addition in the ranges of 80 µM to 120 µM

Figure 13a and Figure 13b display a typical current time response of AgNPGCE modified electrode was assessed by the successive addition of 2 µM glucose concentrations over the range of 2 – 24 µM and 80 – 120 µM respectively into 0.1 M sodium hydroxide at an optimal detection potential of +0.54 V under constant stirring at room temperature. The response time was less than 5s, signifying a facile electron transfer occurred through the AgNPGCE, which displayed well-defined concentration dependence.

The relationship between the steady-state oxidation current with increasing glucose concentration is shown in figure 14a and 14b respectively.

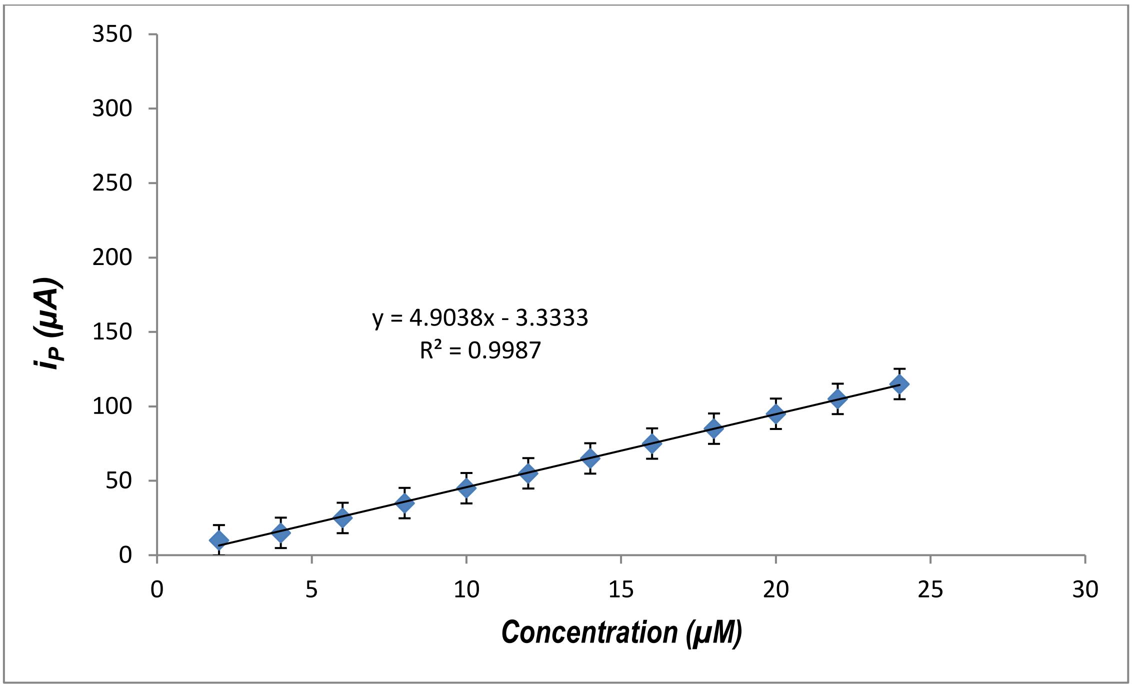

Fig. 14a. Calibration plot of stead–state current versus concentration of glucose

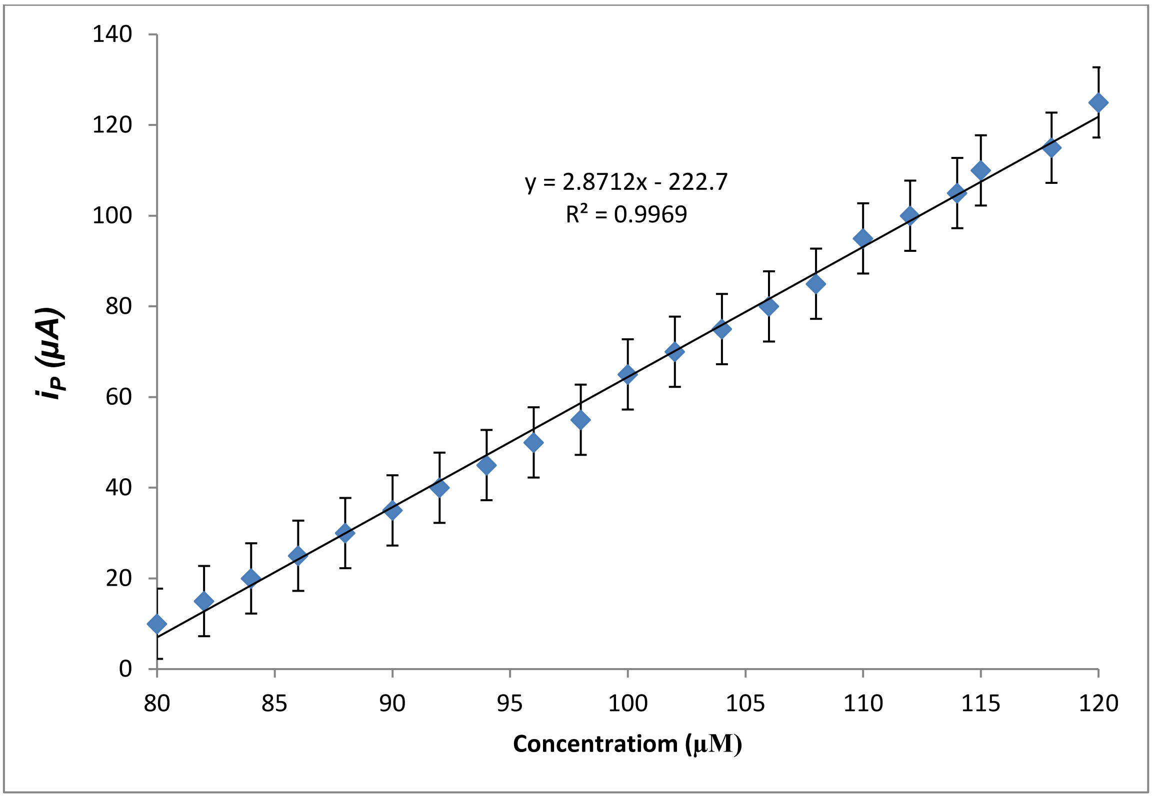

Fig. 14b. Calibration plot of steady–state current versus concentration of glucose

As it shown in figures 14a and 14b above, the current was linear over the glucose concentration range of 2 to 24 µ M with a correlation coefficient of 0.9987. With higher concentrations of glucose, the currents also increased linearly over a wide concentration ranges from 86 to 106 µM. The sensitivity determination is done by dividing the slope from the linearity curve with the surface area of the working electrode used which gave the sensitivity value of 25.02 µ A mM^{-1} cm^{-2} for the modified electrode and the results are presented in table 1.

Table 1. Electrochemical Parameters of AgNPGCE Electrode for glucose sensing in aqueous solution at room temperature

AgNPGCE	**Values**
Heterogeneous electron transfer rate constant (k_e)	6.736 x 10^{-7} cms^{-1}
Charge transfer coefficient (α)	0.54
Sensitivity	25.02 μA/mM/cm^2
Detection limit	1.22 μM
Regression coefficient	0.9987
The surface coverage (ϕ)	3.46 x 10^{-9} $molcm^{-2}$

While the detection limit is obtained from the equation, Detection limit or limit of detection (LOD) $= \frac{(k \times \text{sb})}{\text{m}}$ where k is a constant chosen to be 2 or 3; k value 2 corresponds to a confident level of 92.1% while k value 3 corresponds to a confident level of 98.3%. sb is the standard deviation of the blank and m is the calibration sensitivity which is the slope of the linear plot between concentration and current. The detection limit obtained was found to be 1.22 μM taken k value to be equal 3. This result of the developed AgNPs modified electrode compared favorably well with previously reported enzymatic glucose biosensor [54, 56], suggesting electro-catalytic activity of the silver nanoparticle on glucose, which shows that the working electrode coated with silver nanoparticles has a good ability to measure glucose levels. The non-enzymatic glucose sensors have shown pronounced long-term stability than the enzyme-based glucose sensors.

The eco-friendly stability of the chitosan based silver nanoparticle sensor was examined by keeping in air for three weeks under varying environmental conditions and its sensitivity was examined in accordance with the established procedure and the results are presented in figure 15a and 15b respectively.

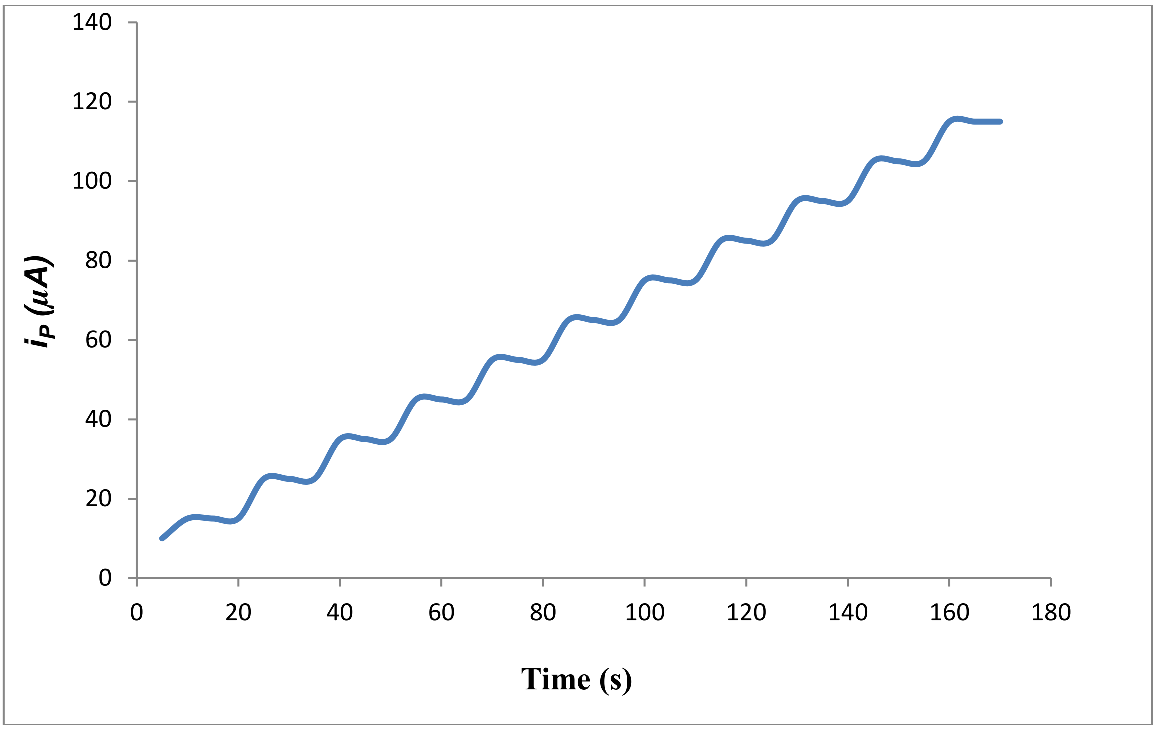

Fig. 15a. Amperometric current versus time curve of silver nanoparticle modified glass carbon electrode (AgNPGCE) for successive glucose addition in the ranges of 2 μM to 24 μM (after being kept in air for two weeks)

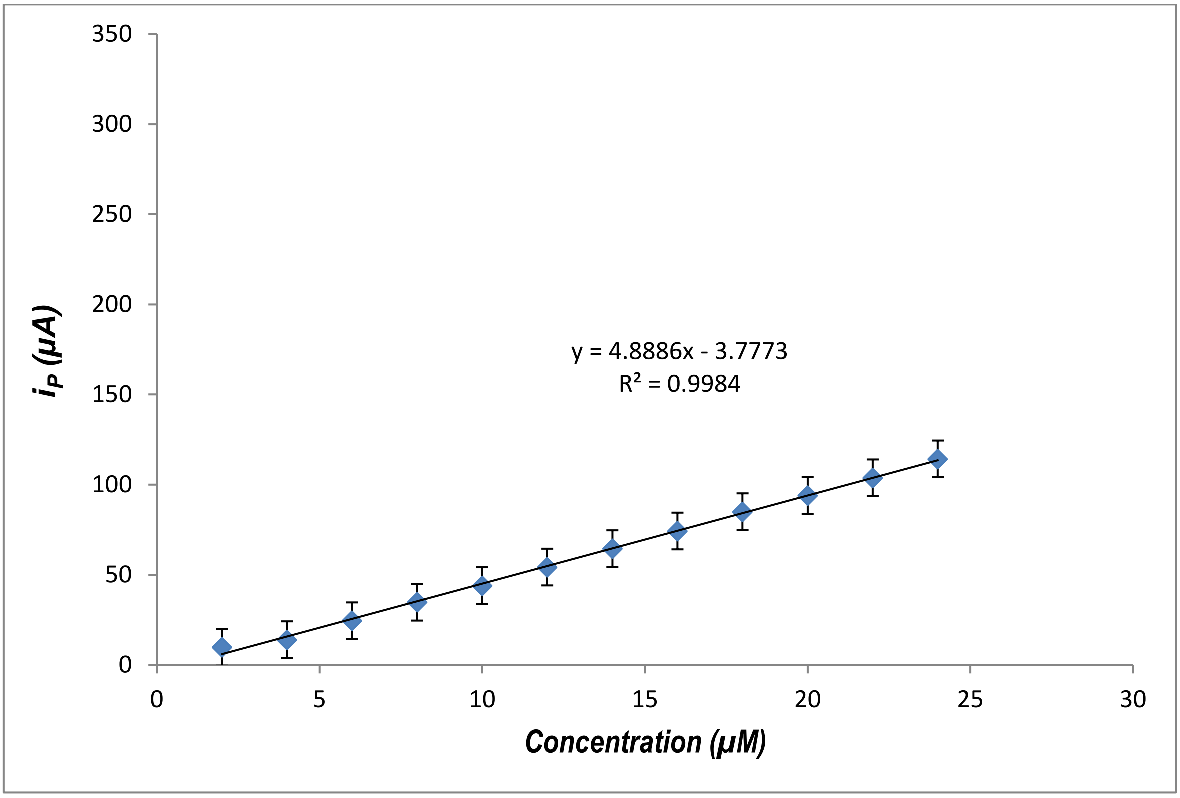

Fig. 15b. Calibration plot of steady–state current versus concentration of glucose

The fabricated silver nanoparticle sensor shows comparable sensitivity of 24.12 $\mu AmM^{-1}cm^{-2}$ which equivalent to 98% of the initial value this demonstrate a very good sensitivity and durability of the sensor for the glucose detection. The good adhesion towards electrode and structural stability of silver nanoparticles could be ascribed to long-term stability. 1.24% relative standard deviation (RSD) with highly reproducible current for eight successive amperometric measurements was gotten for 2 mM glucose on the AgNPGCE electrode. This demonstrates that AgNPGCE electrode can be repeatedly used and the electrode was not infected by the product of oxidation. The highly reproducible mode of fabrication was established with the attainment of 2.48% of RSD using eight electrodes responses measured towards 2 mM glucose.

Conclusion

Silver nanoparticle was prepared and characterized by Fourier transform Infra-red spectroscopy (FTIR), X-ray diffractometry (XRD) and Scanning electron microscopy (SEM). The electro-catalytic activity of the synthesized AgNPs was investigated through potentiometric and amperometric techniques. The crystalline size of the AgNPs was revealed with XRD. The cubic face-centered structure of the synthesized silver nanoparticle was confirmed. This was supported by the observed sharp four diffraction peaks with peaks intense appeared at 2θ = 38.09°, 44.15°, 64.67°, and 77.54°. However, the SEM micrograph of the synthesized AgNPs revealed the spherical shape of AgNPs with a non-uniform granular shape attributed to bio-mediated ionic gelation process. The surface of the synthesized AgNPs has a spherical shape and slightly elongated with a big tendency to aggregate and form larger particle clusters. Whereas, FTIR spectra of AgNPs gave peaks at 1054 – 1645 cm^{-1} suggesting the presence of phosphonate linkages between ammonium, -NH_3^+ of chitosan and –PO_3^{2-} moieties of NaTPP during cross linking process. The electro-catalytic oxidation of glucose at the electrode was examined and the mechanism involved in glucose oxidation was revealed. The silver nanoparticle modified glassy carbon electrode (AgNPGCE) electrode showed a better electrochemical response towards glucose. This glucose sensor shows high sensitivity at +0.54 V. A low detection limit of 1.22 μM taken the confident level k to be 3, and wide linear range of 2 to 24 μM with a correlation coefficient of 0.9987 were obtained. The calculated parameters revealed that AgNPGCE has shown better overall electrochemical performance with a response which compare and compete favorably well with enzymatic biosensor. The fabricated AgNPGCE sensor shows comparable sensitivity (98%) of the initial value, demonstrating the very good sensitivity and durability for the glucose sensing. The long-term stability and reproducibility of the AgNPGCE could be ascribed to the good adhesion of AgNPs towards the electrode and its structural stability.

References

[1] D. Bruen, C. Delaney, L. Florea, D. Diamond, Glucose Sensing for Diabetes Monitoring: Recent Developments, Sensors, 17 (2017) 1866-1872.

[2] S.M. Khor, J. Choi, P. Won, S.H. Ko, Challenges and Strategies in Developing an Enzymatic Wearable Sweat Glucose Biosensor as a Practical Point-Of-Care Monitoring Tool for Type II Diabetes, Nanomaterials, 12 (2022) 221-235.

[3] Z. Yin, Z. Ji, W. Zhang, E.W. Taylor, X. Zeng, J. Wei, The glucose effect on direct electrochemistry and electron transfer reactionnof glucose oxidase entrapped in a carbon nanotube-polymer matrix, Chemistry Select, 5 (2020) 12224–12231.

[4] M. Buaki-Sogó, L. García-Carmona, M. Gil-Agustí, L. Zubizarreta, M. García-Pellicer, A. Quijano-López, Enzymatic Glucose- Based Bio-batteries: Bioenergy to Fuel Next-Generation Devices, Top. Curr. Chem., 378 (2020) 49-58.

[5] M. Güemes, S.A. Rahman, K. Hussain, What is a normal blood glucose? Arch. Dis. Child., 101 (2016) 569-573.

[6] Y. Cheng, X. Gong, J. Yang, G. Zheng, Y. Zheng, Y. Li, Y. Xu, G. Nie, X. Xie, M. Chen, A touch-actuated glucose sensorfully integrated with microneedle array and reverse iontophoresis for diabetes monitoring, Biosens. Bioelectron., 203 (2022) 1140-1156.

[7] I. Rassas, M. Braiek, A. Bonhomme, F. Bessueille, G. Rafin, H. Majdoub, N. Jaffrezic-Renault, Voltammetric glucose biosensor based on glucose oxidase encapsulation in a chitosan-kappa-carrageenan polyelectrolyte complex, Mater. Sci. Eng. C 95 (2019) 152–159.

[8] G. Kaur, A. Kaur, H. Kaur, Review on nanomaterials/conducting polymer based nanocomposites for the development of biosensors and electrochemical sensors, Polym Technol Mater., 60(5) (2021) 502–519.

[9] Q.C. Dong, H. Ryu, Y. Lei, Metal Oxide based non-enzymatic electrochemical sensors for glucose detection, Electrochemical Acta, 2 (2021) 137-144.

[10] Kafi, A.K.M.; Bin Kasri, A.; Jose, R. Glucose Biosensor Based on Glucose Oxidase-Horseradish Peroxidase/Multiporous Tin Oxide (SnO_2) Modified Electrode. J. Nanosci. Nanotechnol., 21 (2021) 3059–3064..

[11] S. Pereira, N. Santos, A. Carvalho, A. Fernandes, F. Costa, Electrochemical Response of Glucose Oxidase Adsorbed on Laser-Induced Graphene, Nanomaterials, 11 (2021) 1893-1906.

[12] R. Bi, X. Ma, K. Miao, P. Ma, Q. Wang, Enzymatic biosensor based on dendritic gold nanostructure and enzyme precipitation coating for glucose sensing and detection. Enzym. Microb. Technol., 162 (2023) 110-122.

[13] N. Shen, H. Xu, W. Zhao, Y. Zhao, X. Zhang, Highly Responsive and Ultrasensitive Non-Enzymatic Electrochemical Glucose Sensor Based on Au Foam. Sensors, 19 (2019) 1203-1217.

[14] F. Zhou, W. Jing, S. Liu, Q. Mao, Y. Xu, F. Han, Z. Wei, Z. Jiang, Electrodeposition of gold nanoparticles on ZnO nanorods for improved performance of enzymatic glucose sensors. Mater. Sci. Semicond., 105 (2020) 1047-1058.

[15] P. Balasubramanian, M. Annalakshmi, S.M. Chen, T.W. Chen, Ultrasensitive Non-Enzymatic Electrochemical Sensing of Glucose in Noninvasive Samples Using Interconnected Nanosheets-like NiMnO3 as a Promising Electrocatalyst. Sens. Actuators, B 299 (2019) 1269-1279.

[16] R. Batool, A. Rhouati, M.H. Nawaz, A. Hayat, J.L. Marty, A Review of the Construction of Nano-Hybrids for Electrochemical Biosensing of Glucose, Biosensors, 9 (**2019**) 46-57.

[17] R. Umapathi, S.M. Ghoreishian, G.M. Rani, Y. Cho, Y.S. Huh, Review-Emerging Trends in the Development of Electrochemical Devices for the On-Site Detection of Food Contaminants, ECS Sensor Plus, 1 (2022a) 574-601.

[18] R. Umapathi, S.M. Ghoreishian, S. Sonwal, G.M. Rani, Y.S. Huh, Portable electrochemical sensing methodologies for on-site detection of pesticide residues in fruits and vegetables. Coord, Chemical Review, 453 (2022b) 284-305.

[19] K.L. Mohamad, N. Nor, N.H. Ramli, H. Poobalan, K. Qi Tan, K. Abdul Razak, Recent Advancement in Disposable Electrode Modified with Nanomaterials for Electrochemical Heavy Metal Sensors, Critical Revieew Analytical Chemistry, 45 (2021) 25-36.

[20] K. Shim, W.C. Lee, M.S. Park, M. Shahabuddin, Y. Yamauchi, S.A. Hossain, Y.B. Shim, J.H. Kim, Au decorated core-shell structured Au@Pt for the glucose oxidation reaction. Sens. Actuators, B 278 (2019) 88−96.

[21] Y.S. Wu, Z.W. Wu, C.L. Lee, Concave Pd core/island Pt shell nanoparticles: Synthesis and their promising activities toward neutral glucose oxidation. Sens. Actuators, B 281 (2019) 1−7.

[22] A.C. Fereshteh Jalilian, K. Sadrjavadi, A. Fattahi, Y. Shokoohinia, Green synthesized silver nanoparticle from Allium ampeloprasum aqueous extract: Characterization, antioxidant activities, antibacterial and cytotoxicity effects, Adv Powder Technol 31 (2020) 1323-1332.

[23] S. Nabavifard, S. Jalili, F. Rahmati, Y. Vasseghian, G.A.M. Ali, Application of Dendrimer/Gold Nanoparticles in Cancer Therapy, A Review. J. Inorg. Organomet. Polym Mater., 30 (2020) 4231-4244.

[24] C.H. Su, C.L. Sun, S.Y. Peng, J.J. Wu, Y.H. Huang, Y.C. Liao, High performance non-enzymatic graphene-based glucose fuel cell operated under moderate temperatures and a neutral solution, J. Taiwan Inst. Chem. Eng. 95 (2019) 48−54,

[25] M. Kiani, N. Rabiee, M. Bagherzadeh, A.M. Ghadiri, Y. Fatahi, Improved Green Biosynthesis of Chitosan Decorated Ag- and Co_3O_4-Nanoparticles: A Relationship Between Surface Morphology, Photocatalytic and Biomedical Applications, Nanomed Nanotechnol Biol Med., 32 (2021) 1023-1031.

[26] J. Khan, K. Saeed, I. Khan, Nanoparticles: Properties, Applications and Toxicities. . Arab J Chem., 12 (2019) 908-931.

[27] B.G. Amin, J. Masud, M. Nath, Non-enzymatic glucose sensor based on $CoNi_2Se_4$/rGO nanocomposite with Ultrahigh sensitivity at low working potential. J. Mater. Chem. B 7 (2019) 2338−2348.

[28] V. Morales-Lozoya, H. Espinoza-Gómez, Z.L. Flores-López, E.L. Sotelo-Barrera, A. Núñez-Rivera, Study of the effect of the different parts of Morinda citrifolia L. (noni) on the green synthesis of silver nanoparticles and their antibacterial activity, Appl. Surf. Sci., 537 (2021) 1478- 1485.

[29] L. Sakalauskiene, A. Popov, A. Kausaite-Minkstimiene, A. Ramanavicius, A. Ramanaviciene, The Impact of Glucose Oxidase Immobilization on Dendritic Gold Nanostructures on the Performance of Glucose Biosensors. Biosensors, 12 (2022) 320-332

[30] R.B. Devika, B.P. Varsha, Studies on Effect of pH on Cross-linking of Chitosan With Sodium Tripolyphosphate: A Technical Note. Pharmaceutical Science Technology, 7(2) (2006) 1-6

[31] M.D. Leonida, S. Banjade, T. Vo, G. Anderle, G.J. Haas, N. Philips, Nanocomposite materials with antimicrobial activity based on chitosan. Inteernational Journal of Nano and Biomaterials, 3(4) (2011) 316-334.

[32] N. Liu, X. Xiang, M. Sun, P. Li, H. Qin, H. Liu, Y. Zhou, L. Wang, L. Wu, J. Zhu, Flexible hydrogel non-enzymatic QCM sensor for continuous glucose monitoring. Biosens. Bioelectron. X 10 (2022) 100-110.

[33] A. Dabhade, S. Jayaraman, B. Paramasivan, Development of glucose oxidase-chitosan immobilized paper biosensor using screen-printed electrode for amperometric detection of Cr(VI) in water, Biotech., 11 (2021) 183-195.

[34] R. Eslami, N. Azizi, S.R. Ghaffarian, M. Mehrvar, H. Zarrin, Highly sensitive and selective non-enzymatic measurement of glucose using arraying of two separate sweat sensors at physiological pH. Electrochim. Acta., 404 (2022) 1397-1412.

[35] H. Wang, W. Zhu, T. Xu, Y. Zhang, Y. Tian, X. Liu, J. Wang, M. Ma, An integrated nanoflower-like MoS_2@$CuCo_2O_4$ heterostructure for boosting electrochemical glucose sensing in beverage. Food Chem., 396 (2022) 1336-1346.

[36] B. Mireia, G. Laura, G. Mayte, G. Marta, Q. Alfredo, Low-Denaturazing Glucose Oxidase Immobilization onto Graphite Electrodes by Incubation in Chitosan Solutions, Polysaccharide, 3 (2022) 388–400.

[37] Borchert, H., Shevchenko, E.V., Robert, A., Mekis, I., Kornowski, A., Grubel, G. and Weller, H. 2005. Silver nanoparticles: Large scale solvothermal synthesis and optical properties. Langmuir, 21, 1931-1936.

[38] Jyoti, K., Baunthiyal, M. and Singh, A. 2016. Characterization of silver nanoparticles synthesized using Urtica dioica Linn. leaves and their synergistic effects with antibiotics. Journal of Radiation Research Applied Science, 9(3), 217–227.

[39] Dubey, S.P., Lahtinen, M. and Sillanpää, M. 2010. Tansy fruit mediated greener synthesis of silver and gold nanoparticles. Process Biochemical, 45(7), 1065–1071.

[40] Ashok, K. T. and Vikas, R. 2010. Cross-linked Chitosan films: Effect of cross-linking Density on swelling parameters. Pakistan Journal of Pharmaceutical Sciences, 23 (4), 443-448.

[41] Kemp, W. 1991. Infrared Spectroscopy. Macmillan Press, London, pp.19-56.

[42] Rekha, M.R. and Sharma, C.P. 2008. pH sensitive succinyl chitosan microarticles: a preliminary investigation towards oral insulin delivery. Trends in Biomaterials & Artificial Organs, 21(2), 107–115.

[43] Modrzejewska, Z., Zarzychi, R. and Sielski, J. 2010. Synthesis of silver nanoparticles in a chitosan solution. Progress on Chemistry and application of chitin, 15, 63-72.

[44] Mallikarjun, K., Narsimha, G., Dillip, G., Praveen, B., Shreedhar, B. and Lakshmi, S. 2011. Green synthesis of silver nanoparticles using Ocimum leaf extract and their characterization. Digest Journal of Nanomaterial Biostructure, 6, 181–186.

[45] Wani, I.A., Ganguly, A., Ahmed, J. and Ahmed, T. 2011. Silver nanoparticles: ultrasonic wave assisted synthesis, optical characterization and surface area studies. Material Letters, 65(3), 520-522.

[46] Vidhu, V.K., Aromal, S. and Philip, D. 2011. Green synthesis of silver nanoparticles using *Macrotylomauniflorum*. Spectrochimica Acta Part A: Molecular and Biomolecular Spectroscopy, 83, 392–397.

[47] F. Sun, X. Wang, Z. You, H. Xia, S. Wang, C. Jia, Y. Zhou, J. Zhang, Sandwich structure confined gold as highly sensitive and stable electrochemical non-enzymatic glucose sensor with low oxidation potential., J. Mater. Sci. Technol., 123 (2022) 113–122.

[48] Baozhan, Z., Guangyue, L., Aiwen, Y., Yanling, X., Martin, M.F. 2014. A sensitive AgNPs/CuOnanofibers non-enzymatic glucose sensor based on electrospinning technology, Sensors and Actuators B: Chemical 195, 431-438.

[49] H.A. Wytse, C. Yejung, S. Kwang-dong, P. Yuanzhe, Simple synthesis of CuO/Ag nanocomposite electrode using precursor ink for non-enzymatic electrochemical hydrogen peroxide sensing, Sensors and Actuators B: Chemical, 255 (2018) 1995-2001.

[50] A.H. Shah, A. Shah, U.A. Rana, S.U.D. Khan, H. Hussain, S.B. Khan, R. Qureshi, B.A. adshah, pH Dependent electrochemical characterization, computational studies of thermodynamic, kinetics and analytical parameters of two phenazine, Electroanalytical, 26 (2017) 2292-2301.

[51] X. Zhang, J. Zhao, C. Wang, L. Zhu, X. Pan, Y. Liu, J. Li, X. Guo, D. Chen, Measurement of sucrose in beverages using a blood glucose meter with cascade-catalysis enzyme particle, Food Chemistry, 398 (2023) 933-951.

[52] Laviron, E. 1979. General expression of the linear potential sweep voltammogram in the case of diffusionless electrochemical systems. Journal of Electroanalytical Chemistry and Electrochemistry, 101, 19–28.

[53] D. Thatikayala, D. Ponnamma, K.K. Sadasivuni, J.J. Cabibihan, A.K. Al-Ali, R.A. Malik, B. Min, Progress of Advanced Nanomaterials in the Non-Enzymatic Electrochemical Sensing of Glucose and H_2O_2. Biosensors, 10 (2020) 151-162.

[54] Wu, S. 2010. Direct electrochemistry of glucose oxidase assembled on graphene and application to glucose detection. Electrochimical Acta, 55(28), 8606-8614.

[55] Chen, J.; Zheng, X.; Li, Y.; Zheng, H.; Liu, Y.; Suye, S.-i. A Glucose Biosensor Based on Direct Electron Transfer of Glucose Oxidase on PEDOT Modified Microelectrode. J. Electrochem. Soc., 167(2020) 675-687.

[56] Z. Yin, Immobilization of Glucose oxidase and Catalase for the Fabrication of Biofuel cell, (2018.) M.Sc. Thesis, North Carolina State University.